Spring 4-2-2018

Characterization of polymers containing ferrocene and imidazole with density functional theory

Eric Mullins
Pittsburg State University, emullins@gus.pittstate.edu

CHARACTERIZATION OF POLYMERS CONTAINING FERROCENE AND IMIDAZOLE WITH DENSITY FUNCTIONAL THEORY

A Thesis Submitted to the Graduate School in Partial Fulfillment of the Requirement for the Degree of Master of Science

Eric Mullins

Pittsburg State University

Pittsburg, Kansas

April, 2018

CHARACTERIZATION OF POLYMERS CONTAINING FERROCENE AND IMIDAZOLE WITH DENSITY FUNCTIONAL THEORY

Eric Mullins

APPROVED:

Thesis Advisor _____
Dr. Ben Tayo, Physics Department

Committee Member _____
Dr. Serif Uran, Physics Department

Committee Member _____
Dr. Charles Neef, Chemistry Department

Committee Member _____
Dr. Khamis Siam, Chemistry Department

ACKNOWLEDGEMENTS

"If I have seen further than others, it is because I have stood upon the shoulders of giants"

-Sir Isaac Newton

There are many people in my life, who I have received unconditional support from in order to be where I am today. Without these people, I would not be able to conduct this research. I would first like to thank my family, for all their support of my pursuit of education. My parents have always been the source of my determination. They have been amazing examples of which to emulate. My brothers and sisters have always been a large source of support to me through their interest in my subject of study. They have always challenged and encouraged me. My instructors have pushed me throughout my academic career to seek out information and challenge myself. While at Pittsburg State University, Dr. Tayo has had a large impact on my education. I have been honored with the opportunity to work with him on this project. His enthusiasm for the subject amazes me, and has encouraged me to pursue further work in this field. I would also like to thank Dr. Uran, Dr. Neef, and Dr. Siam for serving on my thesis committee. They have all taken time out of their busy schedules to help nurture my pursuit of science.

CHARACTERIZATION OF POLYMERS CONTAINING FERROCENE AND IMIDAZOLE WITH DENSITY FUNCTIONAL THEORY

An abstract of the thesis by
Eric Mullins

Electrochemical and UV-Vis studies on these polymers in the presence of aqueous solutions containing metal ions have revealed significant modifications in the electrochemical properties and absorption spectra. These modifications in electrochemical properties could be attributed to the ability of the imidazole to coordinate with metal ions, increasing its electron deficiency and enhancing oxidization of the nearby ferrocene moiety if it is in close proximity with imidazole. However, the mechanism of interaction between the imidazole and metal ions, as well as the equilibrium geometry of the resulting polymer-metal ion complex is unknown.

In this thesis, density functional theory (DFT) was used to study the equilibrium geometry of copolymers containing ferrocene and imidazole. The calculation of equilibrium geometry for molecular systems using DFT is a well- known reliable method that produces trustworthy results within the limits of the theory. With an approximation of two and three polymer segments, equilibrium molecular geometry was obtained as well as the molecular energy levels of the system. Additional calculations of the polymer chains were conducted with sodium atoms bonded to the imidazole group to examine changes in the molecular orbitals. Analysis of these structures showed a shift of the HOMO energy state due to the addition of the sodium atom. Visualization of the density of states plots showed possible correlation with UV-vis experimental results.

TABLE OF CONTENTS

LIST OF TABLES

LIST OF FIGURES

LIST OF ABREVIATION

DFT – Density Function Theory

DOS – Density of States

HOMO – Highest Occupied Molecular Orbital

LUMO – Lowest Unoccupied Molecular Orbital

6-31G – Gaussian basis functions used to mimic atomic orbitals

B3LYP – Model for exchange correlation potential widely used for DFT calculations

LACVP – Basis set that uses effective core potential on larger atoms and 6-31G* for smaller atoms

CHAPTER I

INTRODUCTION

The field of electrochemistry has generated large amounts of interest. A part of this field of research contains organometallic conductors. These conductors are a high area of interest due to understanding charge transfer mechanisms. [1] With the promotion of an electron to an excited state within the conduction band, charge separation is created. This charge separation is created by means of an electron hole pair known as an exciton. [2] This exciton is studied in order to understand the motion of charge on the atomic level.

The charge transfer within the system is created by an electron donor and an electron acceptor. Ferrocene is known to act as an electron donor. [3] The stability of the group allows the group to donate an electron. This is due to the aromaticity of both rings around the iron atom. This aromaticity is what allows an electron to be donated from the system.

The imidazole group also has a high stability due to the resonance structures created by the pi bonds within the five-membered ring. Because of the nitrogen within the imidazole group, a dipole is created. This group exhibits desired characteristics to organometallic conductors due to the group also acting as both an electron donor and acceptor. [4] It is also known that metals coordinate to the nitrogen atom within the

group. The addition of the metal to this group is done to create an increased favorable location for the promotion of an electron.

Experimental studies have been conducted by synthesizing these polymers in the lab. The process in which these are synthesized begins with the addition of methyltriphenylphosphonium bromide to tetrahydrofuran in a nitrogen atmosphere. After substantial mixing, n-butyllithium is added. Finally, ferrocenecarboxadehyde is added to the solution. To produce vinylferrocene. The synthesized vinylferrocene and 1-vinylimidazole are then copolymerized in a nitrogen atmosphere. The final copolymers were placed in different electrolyte solutions for analysis. The spectra taken from which is the basis for the comparison. [5]

Recent electrochemical and UV-Vis studies on these polymers in the presence of aqueous solutions containing metal ions have revealed significant modifications in the electrochemical properties and absorption spectra. [5] These modifications in electrochemical properties could be attributed to the ability of the imidazole to coordinate with metal ions, increasing its electron deficiency and enhancing oxidization of the nearby ferrocene moiety if it is in close proximity with imidazole. However, the mechanism of interaction between the imidazole and metal ions, as well as the equilibrium geometry of the resulting polymer-metal ion complex is unknown.

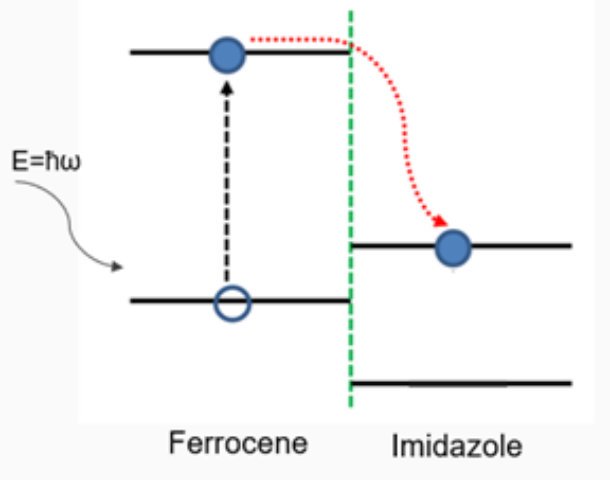

Figure 1: Diagram of charge transfer mechanism

It has been proposed that the proximity of the electron donor-acceptor would create a preferred location for an excited state electron to shift. With this charge separation, the electron hole pair can no longer recombine, and create charge movement across part of the structure. As seen in Figure 1, the excited electron wants to minimize energy states by shifting to the imidazole.

In this thesis, density function theory (DFT) was used to study the equilibrium geometry of copolymers containing ferrocene and imidazole. The analysis is aimed at performing detailed theoretical modeling of the polymer system that could shed useful insights about their equilibrium geometry and provide guidance for interpreting observed spectra. The geometry optimization calculation is accompanied by the calculation of molecular energy levels, hence it produces useful physical quantities such as bond lengths, bond angles, dihedral angles, molecular orbitals, energy gap, and total energy. The charge transfer properties are related to the locations and shapes of the molecular orbitals. It is expected that the addition of metals to the polymer will cause a shift in the

Highest Occupied Molecular Orbital (HOMO) and Lowest Unoccupied Molecular Orbital (LUMO). The results will help characterize the structure of this organometallic conductor, and provide possible insight to the charge transfer process.

CHAPTER II

DENSITY FUNCTIONAL THEORY AND ITS IMPLICATIONS

This analysis aims to solve the Schrodinger equation for a given molecule. Density functional theory (DFT) is a method to approximate a given quantum system. Just like in the approximation of the hydrogen atom, here the Born-Oppenheimer approximation is assumed, where the nucleus is treated as fixed. This assumes the electron is the part of the atom that is in motion. This allows the Schrodinger equation to be used and solve for the energies of the system.

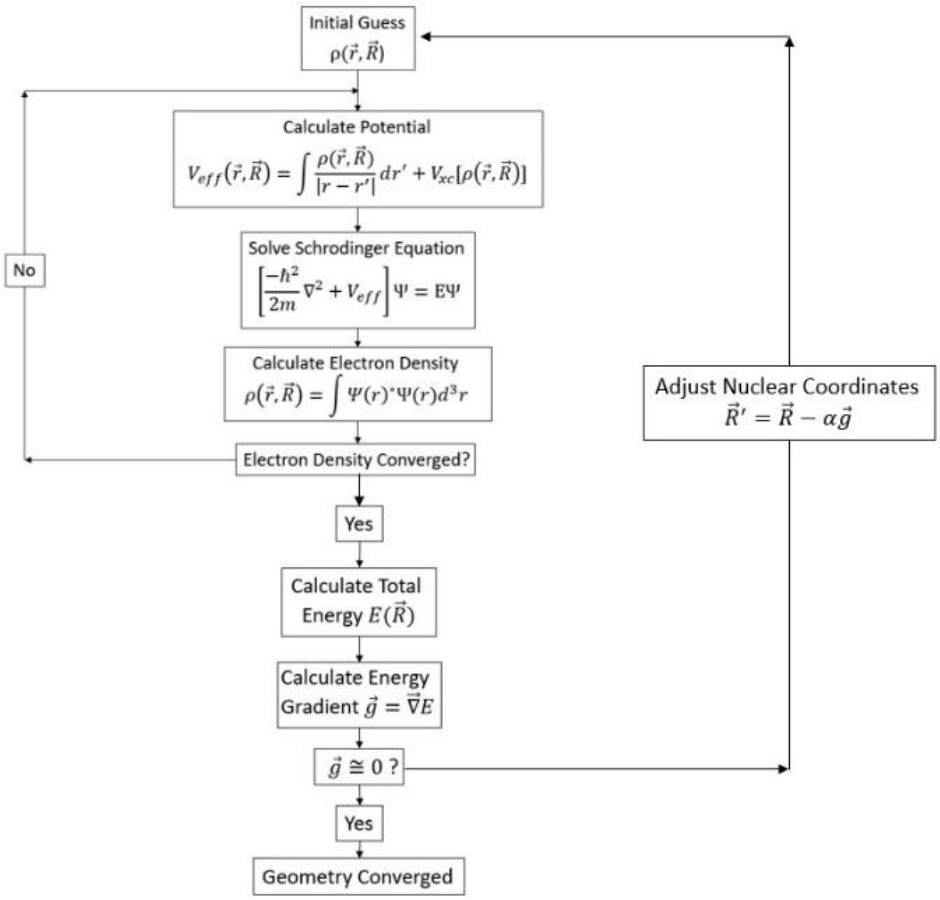

Figure 2: Flow chart for geometry optimization process using DFT

Within the methodology for DFT, a self-consistent field calculation is performed at fixed nuclear coordinates to calculate the converged electron density and total energy. The total energy is then used to calculate the energy gradient, which is used to adjust the relative position vectors of each atom. The process is repeated in a cyclic manner until the total force on each becomes negligible. Figure 2 shows a flow chart of this process. Starting with an initial estimate of the wave function, an electron density can be calculated. Using this initial guess, the effective potential can be calculated for the system. This effective potential is then used to solve the Schrodinger equation. Using the

new calculated wave functions from the Schrodinger equation, the new electron density is calculated. If this electron density is not below the given criteria adjustments are made, and the calculation is repeated. If the electron density is below the threshold, the geometry is adjusted and repeated until convergence. Once this is achieved, values can be obtained from the optimized geometry.

A multi electron system is solved more efficiently with DFT rather than solving the Schrodinger equation for N number of electrons. Instead, this method allows us to start with an initial estimate of the potential, calculating the electron density. The electron density for the system is then used to calculate the wave function, and energy of the system.

$$\rho(\vec{r}) = N \int \psi^*(r)\psi(r)d^3r \qquad (1)$$

Equation 1 is the generalized form relating the electron density ρ to the wave function for N number of electrons. The next sequential step is calculated to minimize the energy of the system until convergence criteria are met. These convergence criteria are set before the calculation begins within the input file. This tells the software to continue optimization iterations until the net force in each individual atom in the structure is below the given value. This means that the structure will lie close to a local energy minimum. How close the structure is to that local minimum depends on how low this set criteria is. Due to computational time constraints, decisions about this value have to be made while also keeping in mind the quality of results. Many different software packages can be used to implement the DFT algorithm and characterize structures. Examples of these programs

are Schrodinger, Gaussian, and GAMESS. In the analysis, results were obtained using the Schrodinger, and GAMESS software packages.

An example of this method is done by optimizing the geometry of the water molecule. This example was conducted using Schrodinger software. The input geometry of water contained a bond angle of 169.24°. For this example, a default convergence criteria of 1.36×10^{-3} eV energy change between steps and the basis set 6-31G* for the atoms. The 6-31G* basis set gives each electron representation within the structure. This approach is accepted for modeling smaller atoms such as oxygen and hydrogen. The energy of the system can then be calculated from the wave functions. The geometry is then slightly shifted, and the energy is then calculated again. This is repeated multiple times until the given convergence criteria is met.

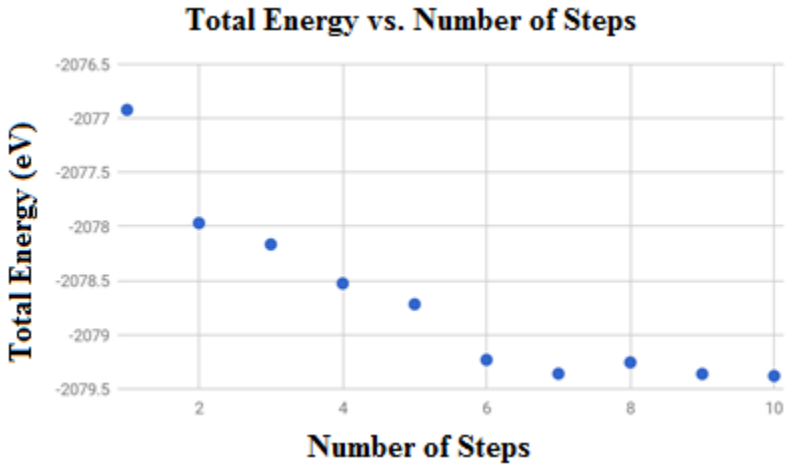

Figure 3: plot of the total energy of the water molecule vs the number of optimization steps

It can be seen in Figure 3, that the total energy of the molecule begins much higher with the initial bond angle. With each step the total energy approaches the minimum energy. At step eight it can be seen that the energy increased slightly, but was accepted to be a bad change since the energy increased. After the equilibrium geometry was achieved, the final geometry can be used to obtain parameters such as bond length, bond angle, and orbital energies. The calculations for water give a final bond angle of 103.68°. Considering that the accepted value for the bond angle of water is 104.5° [6] This shows some similarity to experimentally measured values. From this optimization, the bond length between the oxygen and each hydrogen atom can also be measured. These lengths are 0.966 Å and 0.965 Å. This value has been reported to be approximately 0.96 Å [6] which is very similar to the calculated values. This shows a simple example of how geometrically optimized structures can be used to obtain theoretical measurements of the structure.

The calculation of equilibrium geometry and molecular properties using DFT has been used successfully to model the properties of polymeric systems. [7] Recently, with improvements and advancement in the methodology, DFT has been used to study organometallic systems [3, 8, 9]

This thesis focused on copolymers containing imidazole and their interaction with metal ions. With an approximation of two and three polymer segments, the equilibrium molecular geometry as well as the molecular energy levels of the system was calculated. Additional calculations of the polymer chains are conducted with sodium atoms bonded to the imidazole group in order to examine changes in the molecular orbitals. Molecular

energy levels will be visualized by plotting the density of states (DOS). The molecular orbitals will also be plotted in order to analyze the formation of charge-transfer complexes. Initial geometry was built using Maestro Schrodinger [10] and Avogadro [11] molecular modeling tools. The calculations for the individual monomers were performed using the Schrodinger software [10] installed locally. Calculations for the two and three segments of the polymer were performed using GAMESS [12] software. All computations for the polymers were performed using resources provided by the National Energy Research Scientific Computing Center (NERSC). [13] Post-processing and visualization of molecular orbitals was done using the MacMolPlt software. [14] Calculation of DOS was performed using Mathematica. [15]

CHAPTER III

CHARACTERIZATION OF IMIDAZOLE AND FERROCENE

To provide verifiable standing to the results, a geometry optimization was conducted and the orbital energies for the given monomers were calculated. Using the calculated orbital energy states from the software, the value of the band gap being the difference be the HOMO state and the LUMO state were calculated. To visualize the distribution of molecular energy levels, the density of states (DOS) were plotted. The finite-temperature DOS is given by

$$\rho(E) = \sum_i \frac{\Gamma}{(E-E_i)^2+\Gamma^2} \qquad (2)$$

where E is the energy, E_i are molecular energy levels, and Γ is the linewidth of the Lorentzian spectral function. In this calculation, $\Gamma = 25$ meV which corresponds to the linewidth at room temperature. With the orbital energies found from the software calculations and Equation 2. The equation only returns a result when E is similar in value to Ei. The density of states for the system were plotted.

3.1 OPTIMIZATION OF IMIDAZOLE MONOMERS

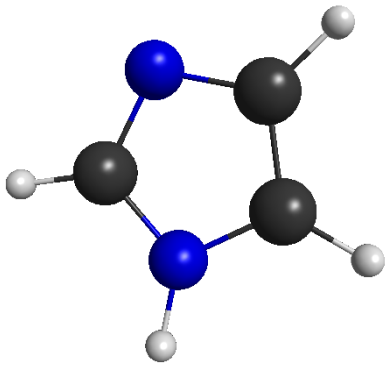

Figure 4: Imidazole, where the blue is hydrogen, grey is carbon, and white is hydrogen

Starting with imidazole, the structure seen in Figure 4 was created using the Schrodinger software. Using a basis set of 6-31G* and the B3LYP level of theory, for the initial calculation of the monomer. This calculation yields a HOMO energy of -6.14 eV and LUMO energy of 0.87 eV.

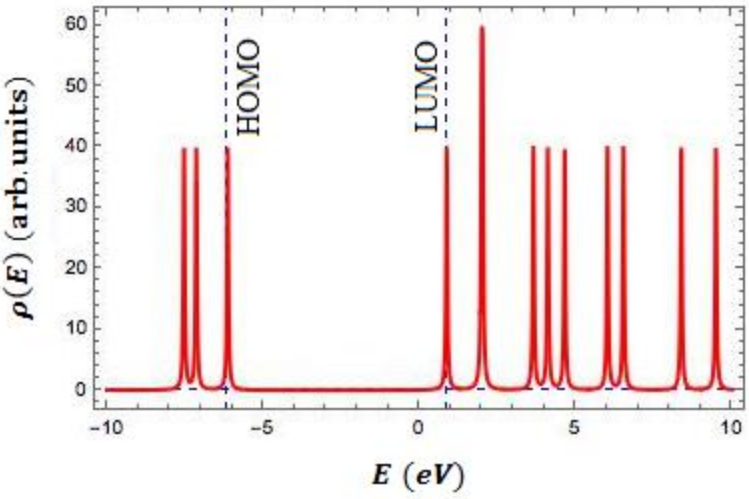

Figure 5: Plot of the density of states for imidazole, showing the band gap. The dotted lines indicate the positions of the HOMO and LUMO energies.

From Figure 5, it is observed that the difference between the energy of the identified HOMO and LUMO states yields a resulting transition energy of 7.01 eV which corresponds to a wavelength of 177 nm. This is close to the measured value of 208 nm, but still contains some discrepancy.

It is often found that the LUMO can be a bad approximation being that the state is unpopulated. In order to create a better approximation, another calculation was conducted using the Schrodinger software, adding an electron to the system. This populates the referred to LUMO state with an electron, possibly giving us a better approximation of the state since the charged structure's HOMO state can be considered close to the neutral structure's LUMO state. Using these values, the new representation of the energy gap can be calculated. [7]

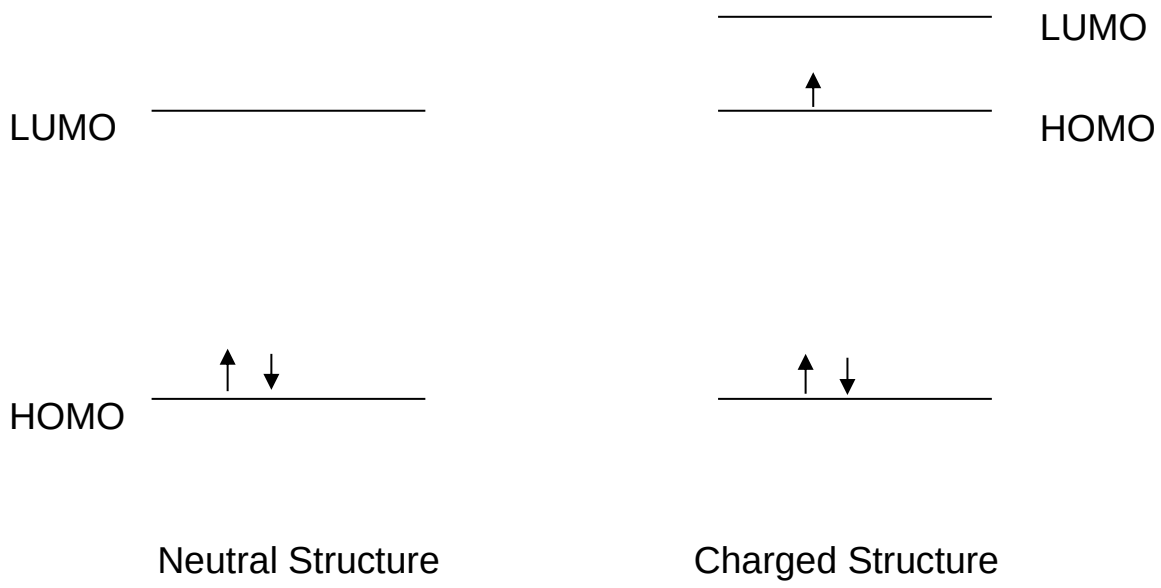

Figure 6: Diagram of the HOMO LUMO states in both the neutral and charged structures

Figure 6 shows a representation of the described approximation. With this adjustment, it was calculated that the charged structure has a HOMO state of 1.34 eV and a LUMO state of 7.73 eV. Using the HOMO state from this calculation as the LUMO state of the neutral structure, an energy gap value of 7.47 eV is obtained, which is 166 nm. In this case, the neutral approximation gave a better result for the energy gap.

A second approximation of the imidazole monomer was attempted using GAMESS. In this calculation, a core potential for the atoms was used. This decreases the calculation time due to only calculating the valence electrons of each atom. With this calculation, a HOMO energy of -6.04 eV and a LUMO energy of 0.74 eV was obtained. This energy results in an energy gap of 6.78 eV or a wavelength of 184 nm. The result is slightly better than the previous findings using the Schrodinger software. As stated, the experimental λ max value has been measured to be 208 nm. [16] This is a fair

approximation for the band gap of the structure, as the experimental results could differ because of band broadening and the theoretical calculations being different than experimental procedures. This would cause a transition at a slightly different energy than predicted due to increased probability of the state.

3.2 OPTIMIZATION OF FERROCENE

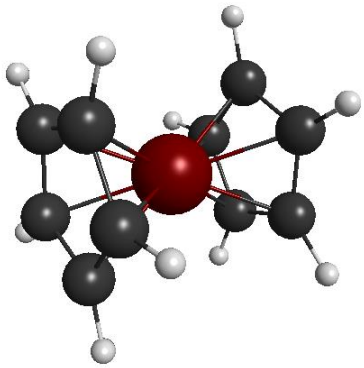

Figure 7: Ferrocene monomer, where red is iron, grey is carbon, and white is hydrogen

Using the same method of analysis, it was found that the ferrocene energy gap of the neutral structure to be approximately 5.20 eV using the Schrodinger software. The optimized geometry can be seen in Figure 7. The ferrocene structure calculations were slightly more complex. Since ferrocene contains an iron atom with a large number of electrons, a basis set for larger atoms was used. The calculations for ferrocene used a pseudopotential basis set of LACVP for the iron atom, and the previous basis set of 6-

31G* for the remaining atoms in the structure. Running the system with the Schrodinger program, a HOMO energy of -5.33 eV and a LUMO energy of -0.03 eV were obtained.

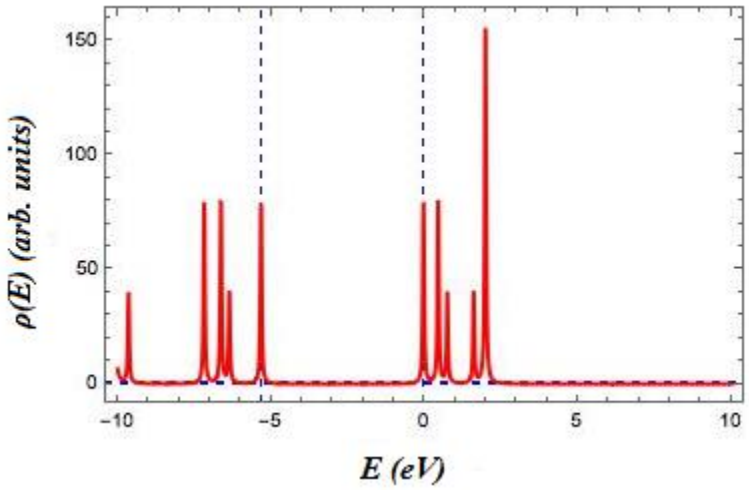

Figure 8: Plot of the density of states for ferrocene, showing the band gap

Calculating the energy gap to be 5.29 eV or 234 nm as seen in Figure 8. Other theoretical studies have reported the energy gap of ferrocene to be in the range 4.26 eV to 5.76 eV. [8] Hence the calculated energy gap of 5.29 eV is acceptable.

To again improve the LUMO calculation for the system, the same structure using the same basis set with an extra electron in the system was calculated. In doing so, a HOMO energy state of 0.90 eV and LUMO energy state of 3.68 eV were obtained. Using the HOMO value as the LUMO approximation as previously conducted, the energy gap was calculated to be 6.23 eV or 199 nm. This once again makes the monomers approximation worse than the neutral structure calculation.

Finally, the ferrocene structure was calculated on the GAMESS system for a comparison of values. This calculation yielded a HOMO energy of -5.28 eV and a LUMO energy of -0.05 eV. Resulting in a band gap value of 5.22 eV. Again, the value of 4.20 eV could differ since it is found through experimental data and the use of a solvent. The optimized structure in the approximation can also be checked with known experimental measurements of the distance between the iron atom and any carbon atom on the rings. Within the calculations using GAMESS, an iron to carbon atoms bond length of 2.08 Å was obtained. The experimental distance between iron and the carbon atoms is 2.064 ± 0.003 Å. [17] These two measurements are very similar.

Overall, both methods show a basic approximation for the monomers used in the polymer. The calculations could differ from the experimental values due to the exclusion of solvents, but show strong reliability for analytical purposes.

CHAPTER IV

CHARACTERIZATION OF POLYMERS CONTAINING FERROCENE AND IMIDAZOLE

Using the Schrodinger software, the monomer groups of both ferrocene and imidazole were built. The Schrodinger software contains a polymer builder that was used to build the polymer chains.

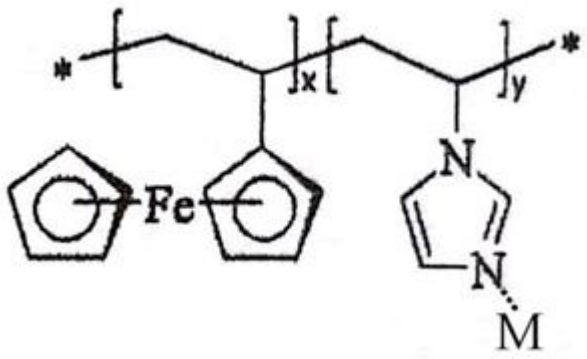

Figure 9: One polymer segment containing ferrocene and imidazole where M is a metal ion, e.g. Na^+

As seen in Figure 9, single segment's length contains both ferrocene and imidazole. Ideally, a polymer chain would be infinitely long. However, due to limits on computational time, the analysis was conducted on smaller segments. Chains were

created of two, and three segments for the calculations using the Schrodinger software. Software was then used to generate optimization input files for the GAMESS software. The calculations were executed using time on a supercomputer at the National Research Scientific Computing Center (NERSC). [13] With this resource available, computational time was decreased on the larger structures. Similar to the monomer analysis, the calculations were done using the core potentials in the GAMESS software. Additional changes such as damping were added in order to allow the structure to converge within the allotted number of steps for a self-contained field calculation. This damping effect creates some change in the final results, but is minimal.

4.1 TWO-SEGMENT MODEL OF THE POLYMER

By examining the two segment structure with the ferrocene and imidazole groups with no addition of metals an initial analysis was made. This two segment polymer was calculated using a core potential basis set. The convergence criteria used was a value of 0.02 eV/Å.

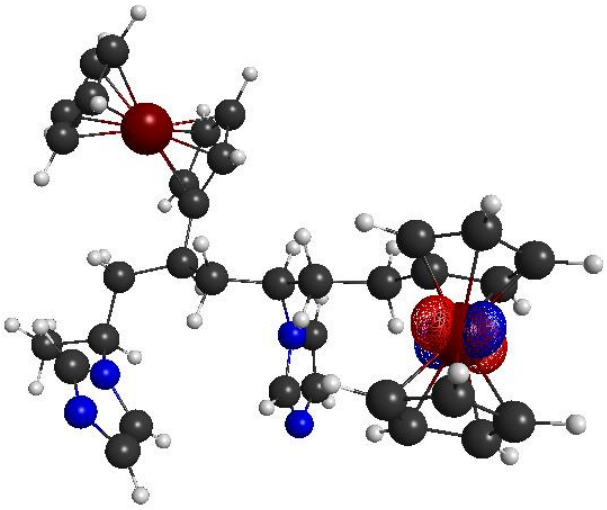

Figure 10: Two segment polymer optimized structure containing no metal atoms bonded to imidazole, HOMO orbital plotted.

With the final optimized structure, it can be seen that the ferrocene groups attempt to spread out in order to reduce spatial interference between the two groups. The two imidazole groups remain close together on the same side. In Figure 10, the HOMO orbital is localized to the iron atom on a single ferrocene group. The LUMO orbital looks identical to the HOMO orbital, only on the other ferrocene group. This orbital trend continues until a higher molecular orbital was reached.

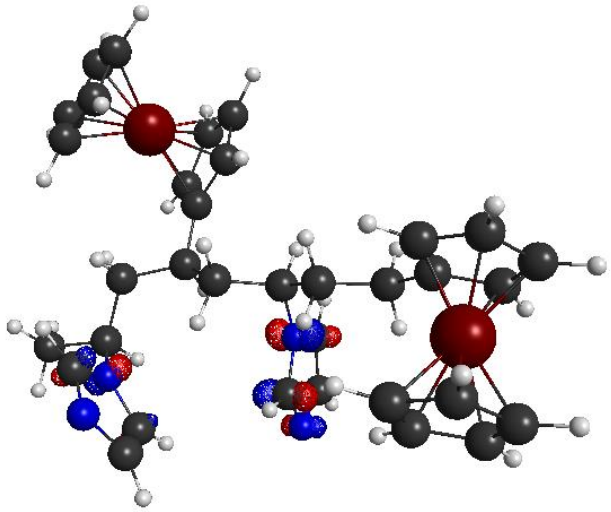

Figure 11: Two segment polymer optimized structure containing no metal atoms bonded to imidazole, LUMO +4 orbital plotted.

Since the LUMO orbital showed similar shape around the other ferrocene group, the other orbitals in the conduction band were examined. These all show similar orbitals around the iron atoms within the ferrocene group until the LUMO +4 orbital. Seen plotted in Figure 11, this molecular orbital shows delocalization across both imidazole groups. The LUMO +5 molecular orbital also shows the same characteristics of delocalization across both imidazole groups.

Table 1: Energy gap calculations for two segment polymer at varying concentrations of Na.

Na concentration	HOMO(eV)	LUMO(eV)	Egap (eV)
Zero Na atoms	-5.31	-0.41	4.90
One Na atom	-10.45	-2.15	8.29
Two Na atoms	-14.59	-4.68	9.90

With the addition of sodium atoms to the structure, it can be seen that increasing the number of sodium atoms within the structure, the HOMO energy becomes more negative as seen in Table 1. The HOMO energy is related to the binding energy of the valence electrons. This more negative value seems reasonable due to the polymer charge increasing by +1 for every sodium atom, thus making the system more difficult to remove an electron.

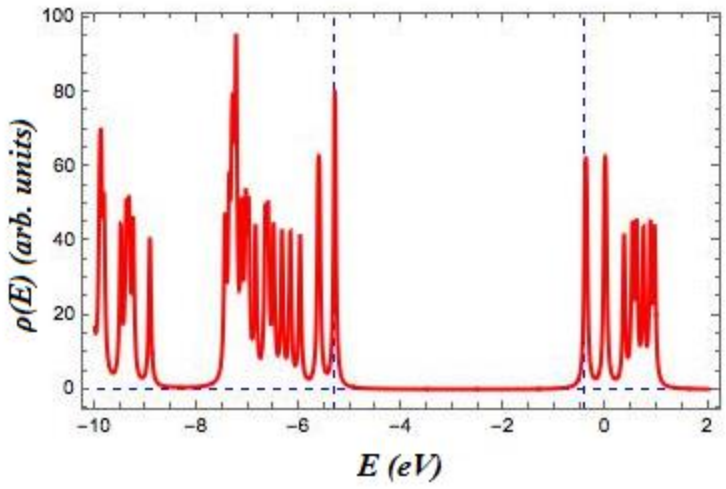

Figure 12: Density of states for two segment polymer containing no metal atoms attached to imidazole group.

By plotting the density of state, it is possible conclusions of different transitions. It can seen with the band gap of 4.90 eV, this would correspond to a spectrum wavelength of 253 nm. This peak has not been observed in experimental UV-vis spectrum data due to limitations of the experimental equipment. Examining the density of states for the polymer containing no added metal atoms seen in Figure 12, that there is a smaller additional band gap within the valence states of about 1.47 eV. The observed UV-vis spectral peak around 450 nm [5] could be attributed to one of these transitions across the gap in the upper part of the valence states. Once one of the electrons is promoted from the valence band to the conduction band, an empty state is left within the valence band. This makes another transition possible from a lower state to this unoccupied valence state.

To approximate the polymer in a sodium electrolyte solution, sodium atoms were added to the nitrogen atom within the imidazole group as seen in Figure 9. This imidazole group acts as a Lewis base, donates a pair of electrons to the metal. To examine different

concentrations of the electrolyte solution, varying amounts of sodium atoms were added to the polymer chain for analysis.

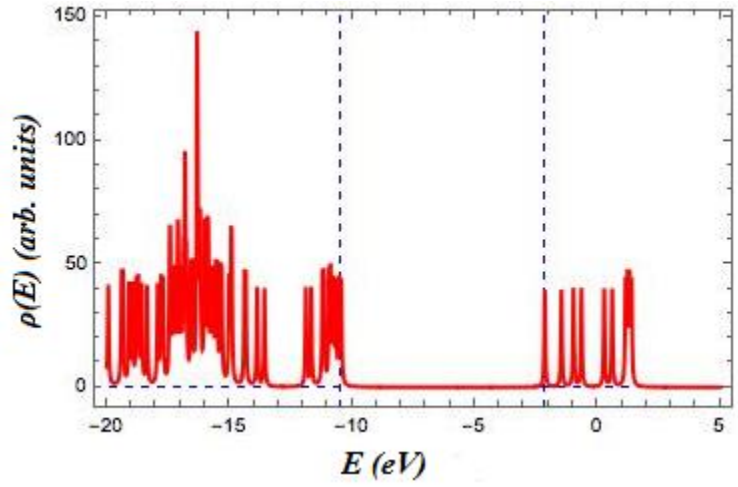

Figure 13: Density of states for two segment polymer with one Na atom.

The addition of one sodium atom appears to widen the band gap of the system as seen in Figure 13. However, this does not seem to alter the smaller gap within the valence band compared to Figure 12. As previously stated, this could be the cause of the observed peak in the UV-vis spectrum data.

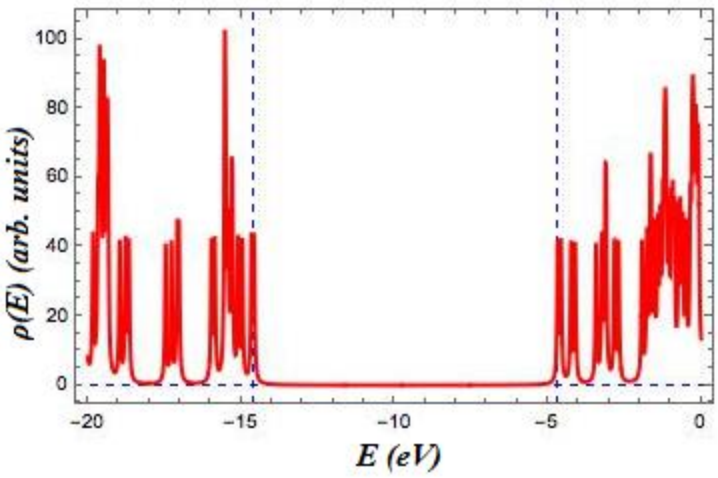

Figure 14: Density of states for two segment polymer with two Na atoms

With the addition of another sodium atom to the system, an increase in the size of the band gap is observed. The second sodium atom seems to significantly alter the density of states within the valence band. This shift in states seems to further support the idea that previous spectrum data is observing smaller transitions within the valence band system due to a second gap in states being formed seen in Figure 14.

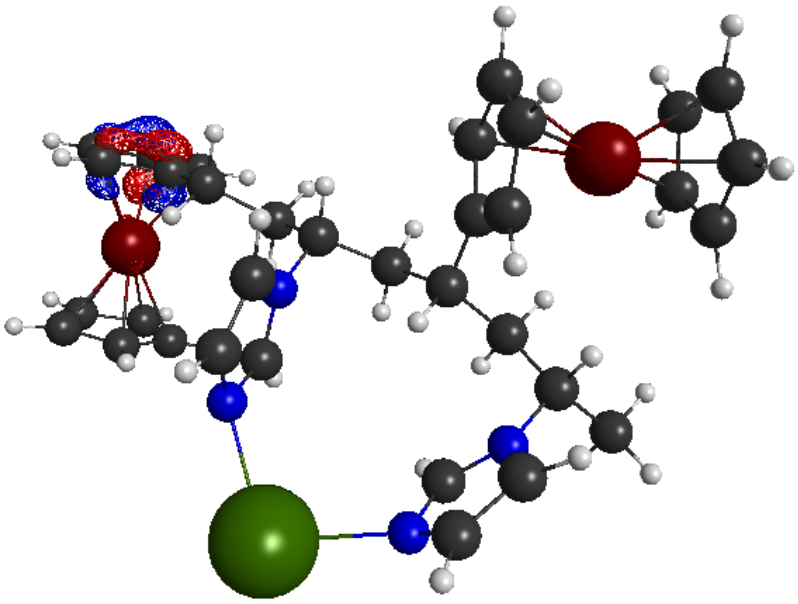

Figure 15: Two segment polymer optimized structure containing one sodium atom bonded to imidazole groups, HOMO orbital plotted.

With the addition of one sodium atom bonded to a single imidazole group, the minimized geometry structure was obtained when the adjacent imidazole group is also bonded to the sodium atom. Considering that the sodium atom only needs two electrons to fill its valence orbital, it is possible to assume that a resonance structure has been created between the two imidazole groups and the sodium atom. This claim is supported by the geometry of the optimized structure being very symmetric. The bond length between the sodium atom and nitrogen atoms are 2.41 Å and 2.41 Å with a bond angle of 38.69°. These similar bond lengths show how the sodium is shared between the two

imidazole groups. With the addition of this sodium atom, a shift in the HOMO orbital was observed. As seen plotted in Figure 15, the HOMO orbital has now shifted from the iron atom in the ferrocene to a more delocalized orbital across part of the aromatic ring and the iron atom. The LUMO orbital is highly localized to the sodium atom.

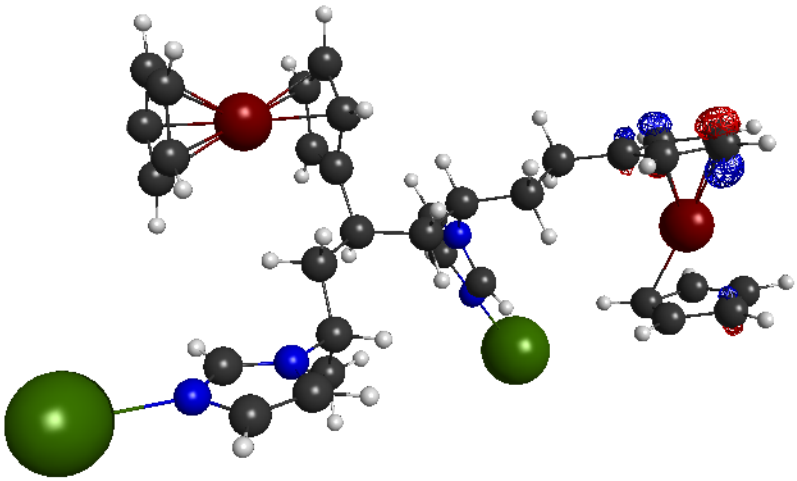

Figure 16: Two segment polymer optimized structure containing two sodium atoms bonded to imidazole groups, HOMO orbital plotted.

With the addition of a sodium atom on each of the imidazole groups, a different optimized structure is obtained. The addition of this second sodium atom, the two imidazole groups want to shift away from the other due to the increased charge. Similar to the one sodium addition, the HOMO orbital seen in Figure 16 is delocalized across the

aromatic ring of the ferrocene. The LUMO orbital is again localized to the adjacent sodium atom. The bond length of the sodium with nitrogen within the imidazole group is approximately 2.41 Å for both segments. This is consistent with the previous calculations with a single sodium addition.

4.2 THREE-SEGMENT MODEL OF THE POLYMER

Table 2: Energy gap calculations for three segment polymer at varying concentrations of Na.

Na concentration	HOMO(eV)	LUMO(eV)	Egap(eV)
Zero Na atoms	-5.28	-0.46	4.82
One Na atom	-9.55	-3.37	6.18
Two Na atoms	-10.83	-4.90	5.93
Three Na atoms	-12.54	-6.78	5.76

A similar analysis was conducted with a three segment polymer, the data can be found in Table 2. With the increase in the number of atoms, the convergence criteria was loosened in order to obtain results within a reasonable length of time. For the three segment optimizations, a convergence criteria of 0.23 eV/Å. This convergence criteria was chosen due to problems with the large system of electrons converging within a set

number of self-contained field steps. The polymer with no added sodium atoms returned similar results to the two segment. While the HOMO state is still located on the iron atom as before, the orbital is now slightly delocalized across another ferrocene group. The LUMO state also shows this same characteristic of localization to the iron atom, which is consistent with the two segment no sodium results. With this data, the increasing negative value for the HOMO orbital is still observed. This is consistent with the two segment analysis. With this shorter analysis, we see a small decrease in band gap size with the addition of more sodium atoms.

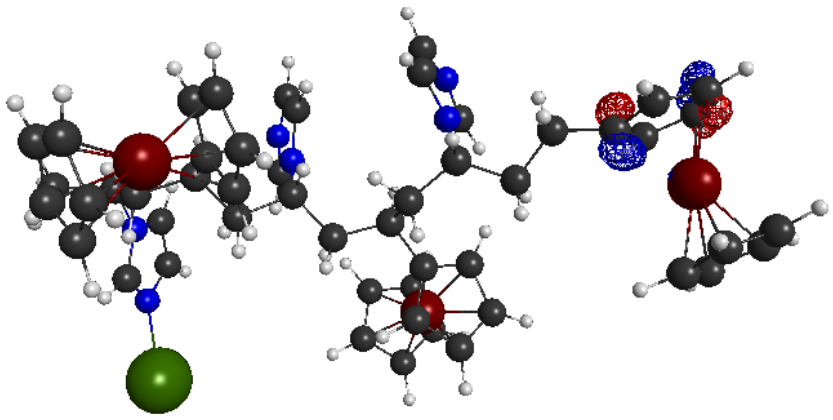

Figure 17: Three segment polymer optimized structure containing one sodium atom bonded to imidazole group, HOMO orbital plotted.

Examining the optimized structure, there are many similarities with the previous analysis. The addition of the sodium atom has again shifted the HOMO orbital to the aromatic ring system with one of the ferrocene groups seen in Figure 17. The LUMO orbital is again highly localized to the sodium atom. Some characteristics of the structure show the drawbacks to this shorter optimization. The bond length between the sodium and nitrogen in the imidazole group has now be calculated to be 2.37 Å, showing some difference from the previously calculated result.

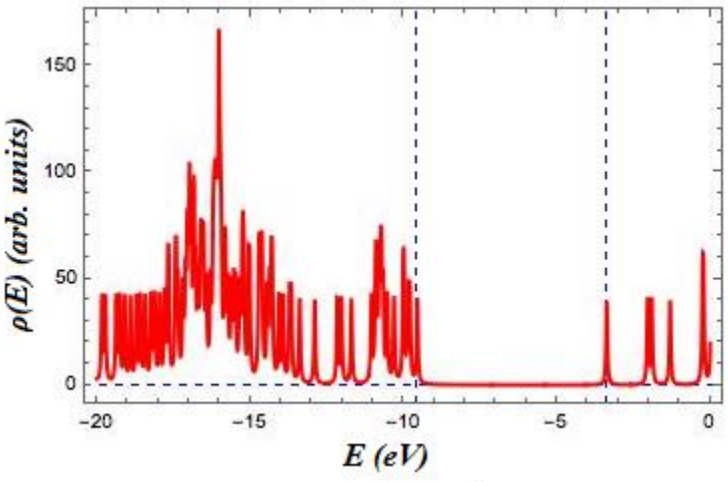

Figure 18: Density of states for three segment polymer with one Na atom

Similar to the two segment analysis, a small spacing of states in the upper part of the valence band is seen. With this analysis, in Figure 18 it is seen that the one sodium addition has a band gap of approximately 6.18 eV.

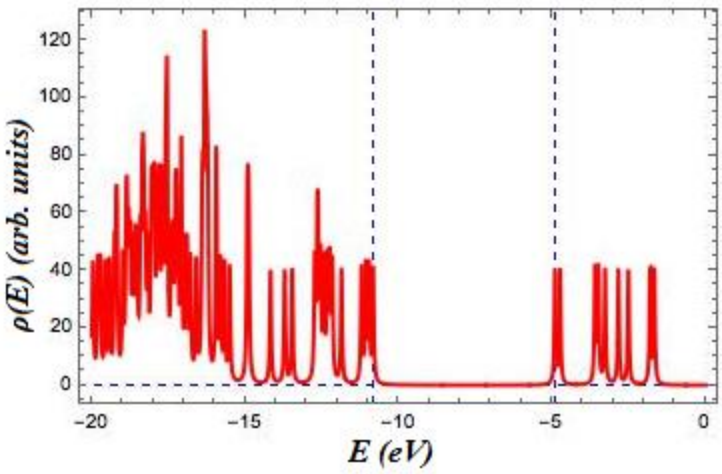

Figure 19: Density of states for three segment polymer with two Na atoms

With an increase in the concentration of sodium atoms in the three segment polymer, the characteristics of small band gaps within the upper regions of the valence states are retained. In Figure 19 there are a large number of valence states with similar orbital energies just below the small band gaps.

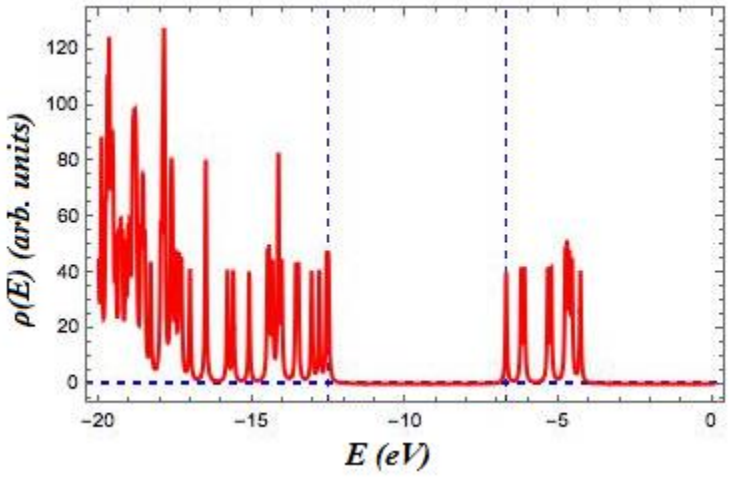

Figure 20: Density of states for three segment polymer with three Na atoms

Increasing the concentration of the sodium atoms again, the upper valance states retain their previous pattern, as seen in Figure 20. This result agrees with the two segment polymer analysis.

CHAPTER V

CONCLUSIONS AND PERSPECTIVES

With the density functional approximations, the structure of the polymer was characterized. Insight into the electrochemical properties by examining the molecular orbitals was obtained. With the given structures of the polymer, it seems apparent that the promotion of an electron in the system will shift charge from the ferrocene group to the imidazole group, thus providing a means of charge transfer across the polymer structure. The analysis could differ from experimental findings due to the calculations being conducted in the gas phase rather than in solution with a solvent.

The DOS plots for the structures showed a trend of small gaps in the upper parts of the valence band. It was hypothesized that this could be the source of observed spectra data due to the band gap appearing in all of the DOS plots. This band gap value is similar to the experimentally observed wavelength, but shows a slightly smaller value. Time dependent calculations could be conducted to see which transition has the largest probability of occurring. It is possible that a transition from a similar state close to the band gap within the upper parts of the valence band would cause the observed wavelength if it is a more probable transition.

Additional computational time for longer segments and better convergence could be done to improve the results. While the three segment structure shows similar trends to the better converged two segment analysis, the geometry was not fully optimized for the larger approximation. With the addition of one and two sodium atoms on the three segment polymer, a bond length was achieved between the sodium and nitrogen atom similar to the two segment. However, at this level of convergence, the imidazole group did not attempt to rotate and create a resonance structure like the two segment analysis.

REFERENCES

[1] J. K. Kochi, "Charge-transfer excitation of molecular complexes in organic and organometallic chemistry," *The Scientific Journal of IUPAC,* pp. 255-264, 2009.

[2] A. Chernikov, T. C. Berkelbach, H. M. Hill, A. Rigosi, Y. Li, O. B. Aslan, D. R. Reichman, M. S. Hybertsen and T. F. Heinz, "Non-Hydrogenic Exciton Rydberg Series in Monolayer WS2," *Physical Review Letters,* 2014.

[3] A. Alzharani, C. Ault, E. Allehyani, C. S. Hance, R. Westby, B. O. Tayo, and C. J. Neef, "Electrochemical studies of ferrocene and maleimide containing alternating copolymers," *Journal of Electroanalytical Chemistry,* pp. 129-134, 2017.

[4] K. Kreuera, "Imidazole and pyrazole-based proton conducting polymers and liquids," *Science Direct,* pp. 1281-1288.

[5] A. S. Alhathir, "Synthesis and Electrochemical Study of Copolymers Containing Ferrocene and Imidazole," 2017.

[6] A. Hoy and P. Bunker, "A precise solution of the rotation bending Schrodinger equation for a triatomic molecule with application to the water molecule," *Journal of Molecular Spectroscopy,* pp. 1-8, 1979.

[7] T. M. McCormic, C. R. Bridges, E. I. Carrera, P. M. DiCarmine, G. L. Gibson, J. Hollinger, L. M. Kozycz and D. S. Seferos, "Conjugated Polymers: Evaluating DFT MEthods for More Accurate Orbital Energy Modeling," *Macromolecules,* pp. 3879-3886, 2013.

[8] Y. Yuan and L. Cheng, "Ferrocene analogues of sandwich B12-Cr-B12: A theoretical study," *The Journal of Chemical Physics,* 2013.

[9] S. M. Tekarll, M. L. Drummond, G. T. Williams, T. R. Cundarl and A. K. Wilson, "Performance of Density Functional Theory for 3d Transistion Metal-Containing Complexes: Utilization of the Correlation Consistent Basis Sets," *Journal of Physical Chemistry,* pp. 8607-8614, 2009.

[10] *Bochevarov, A.D.; Harder, E.; Hughes, T.F.; Greenwood, J.R.; Braden, D.A.; Philipp, D.M.; Rinaldo, D.; Halls, M.D.; Zhang, J.; Friesner, R.A., "Jaguar: A high-performance quantum chemistry software program with strengths in life and materials sciences," I.*

[11] *Avogadro: an open-source molecular builder and visualization tool. Version 1.2.0 http://avogadro.cc/.*

[12] *General Atomic and Molecular Electronic Structure System" M.W.Schmidt, K.K.Baldridge, J.A.Boatz, S.T.Elbert, M.S.Gordon, J.H.Jensen, S.Koseki,*

N.Matsunaga, K.A.Nguyen, S.Su, T.L.Windus, M.Dupuis, J.A.Montgomery J. Comput. Chem., 14, 1347-1363(1993).

[13] *National Energy Research Scientific Computing Center, a DOE Office of Science User Facility supported by the Office of Science of the U.S. Department of Energy under Contract No. DE-AC02-05CH11231..*

[14] *Bode, B. M. and Gordon, M. S. J. Mol. Graphics Mod., 16, 1998, 133-138..*

[15] *Mathematica, Version 9.0 (Wolfram Research, Inc, Champaign, IL, 2012).*

[16] M. K. Trivedi, A. Branton, D. Trivedi, G. Nayak, G. Saikia and S. Jana, "Physical and Structural Characterization of Biofield Treated Imidazole Derivatives," *Natural Products Chemistry & Research,* vol. 3, no. 5, 2015.

[17] A. Haaland and J. E. Nilsson, "The Determination of Barriers to Internal Rotation by Means of Electron Diffraction. Ferrocene and Ruthenocene," *ACTA CHEMICA SCANDINAVICA,* no. 22, pp. 2653-2670, 1968.

APPENDIX

SAMPLE BATCH FILE

```
#!/bin/bash -l
#SBATCH -J polytwoN
#SBATCH -q regular
#SBATCH -N 2
#SBATCH -C haswell
#SBATCH -t 24:00:00

cd $SLURM_SUBMIT_DIR
module load gamess

rungms-xt polysegtwoNthree.inp 32 16
```

SAMPLE INPUT FILE

```
!  File created by the GAMESS Input Deck Generator Plugin for Avogadro
 $BASIS GBASIS=N31 NGAUSS=6 NDFUNC=1 $END
 $CONTRL SCFTYP=RHF RUNTYP=OPTIMIZE DFTTYP=B3LYP MAXIT=200
$END
 $SCF DIRSCF=.TRUE. SOSCF=.TRUE. DAMP=.TRUE. CONV=0.0001 $END
 $SYSTEM MWORDS=125 $END
```

$STATPT OPTTOL=0.00045 NSTEP=200 $END

$DATA

Title

C1

H	1.0	-1.85002	1.66419	-2.23205
C	6.0	-0.03356	2.30269	-3.19167
C	6.0	1.32383	2.86299	-2.91327
C	6.0	1.42377	4.13601	-3.43227
C	6.0	0.23716	4.48261	-4.03742
C	6.0	-0.65857	3.44171	-3.92550
C	6.0	2.42494	0.55943	-6.27164
C	6.0	0.97344	0.22873	-6.30388
C	6.0	0.48805	1.20445	-7.31896
C	6.0	1.53478	1.97910	-7.77111
C	6.0	2.69630	1.59218	-7.14302
Fe	26.0	0.15117	0.71059	-4.48081
C	6.0	-0.81933	1.94437	-1.92509
C	6.0	-0.18803	0.76472	-1.16824
H	1.0	-0.87913	2.83275	-1.25749
H	1.0	0.85071	1.02652	-0.87334
H	1.0	-0.14620	-0.11684	-1.84557

N	7.0	-2.37538	0.08691	-0.21874
C	6.0	-2.83032	-0.89767	-1.01933
C	6.0	-3.46667	0.73005	0.23080
C	6.0	-4.57408	0.11451	-0.30866
N	7.0	-4.17696	-0.90641	-1.09419
C	6.0	-0.97954	0.41234	0.11107
C	6.0	-0.30354	-0.77468	0.85470
H	1.0	-3.46015	1.57952	0.90156
H	1.0	-5.60591	0.39211	-0.14086
H	1.0	-0.97107	1.31483	0.73396
H	1.0	0.75117	-0.54484	1.12031
H	1.0	-0.28258	-1.55543	0.08994
C	6.0	-0.93082	-0.45116	3.39886
C	6.0	-2.01611	-0.78522	4.38615
C	6.0	-2.74452	0.33806	4.70639
C	6.0	-2.22640	1.42254	4.04588
C	6.0	-1.15611	1.02379	3.27804
C	6.0	1.89308	-0.78887	7.00370
C	6.0	2.30379	-1.37098	5.69706
C	6.0	3.41203	0.21008	5.70388
C	6.0	2.07491	1.40187	6.07146
C	6.0	1.78743	0.58005	7.14206

Fe	26.0	0.89505	-0.77878	4.30564
C	6.0	-1.06225	-1.32926	2.10236
C	6.0	-0.55433	-2.76044	2.49012
H	1.0	-2.13792	-1.41294	1.83530
H	1.0	-1.05709	-3.03523	3.43799
H	1.0	0.53621	-2.72984	2.70663
N	7.0	-0.15841	-3.90915	0.26763
C	6.0	1.17775	-3.88313	0.07975
C	6.0	-0.70264	-3.91489	-0.96220
C	6.0	0.32268	-3.87884	-1.88070
N	7.0	1.50306	-3.85930	-1.22885
C	6.0	-0.88654	-3.94976	1.54050
C	6.0	-0.56017	-5.27815	2.23852
H	1.0	-1.76309	-3.94395	-1.17565
H	1.0	0.21754	-3.87104	-2.95723
H	1.0	-1.98271	-3.94651	1.34620
H	1.0	-1.14136	-5.37875	3.17986
H	1.0	0.52235	-5.34319	2.47936
H	1.0	-0.83006	-6.12773	1.57549
H	1.0	-0.54868	1.71632	2.71881
H	1.0	-2.57258	2.44314	4.13867
H	1.0	-3.57432	0.35814	5.39975

H 1.0 -2.21923 -1.75691 4.81366

H 1.0 2.29673 -2.47837 5.77354

H 1.0 1.47745 1.00781 8.08712

H 1.0 1.99847 2.47647 6.16958

H 1.0 4.12545 0.62429 5.01279

H 1.0 1.66157 -1.43590 7.84078

H 1.0 0.79242 -0.82169 -6.61338

H 1.0 3.16272 0.07936 -5.64287

H 1.0 3.67357 2.03024 -7.29557

H 1.0 -0.53793 1.31237 -7.64433

H 1.0 1.44536 2.77279 -8.50069

H 1.0 2.30848 4.75546 -3.37767

H 1.0 2.12791 2.35121 -2.40193

H 1.0 0.03262 5.41965 -4.53721

H 1.0 -1.66169 3.45145 -4.33153

H 1.0 -2.19799 -1.59544 -1.54724

H 1.0 1.90714 -3.87823 0.87894

$END